

Pressure-based Detection of Heart and Respiratory Rates from Human Body Surface using a Biodegradable Piezoelectric Sensor

Ziqiang Xu¹, Akira Furui¹, Shumma Jomyo¹, Toshiki Sakagawa¹,
 Masanori Morita², Tsutomu Takai², Masamichi Ando², and Toshio Tsuji¹

Abstract—This study investigates the relationship between respiration and autonomic nervous system (ANS) activity and proposes a parallel detection method that can simultaneously extract the heart rate (HR) and respiration rate (RR) from different pulse waves measured using a novel biodegradable piezoelectric sensor. The synchronous changes in heart rate variability and respiration reveal the interaction between respiration and the cardiovascular system and their interconnection with ANS activity. Following this principle, respiration was extracted from the HR calculated beat-by-beat from pulse waves. Pulse waves were measured using multiple biodegradable piezoelectric sensors each attached to the human body surface. The Valsalva maneuver experiment was conducted on seven healthy young adults, and the extracted respiratory wave was compared with a reference respiratory wave measured simultaneously. The experimental results are consistent with the observations from reference waves, where $R^2 = 0.9506$, $p < 0.001$ for the extracted RR and the reference RR, thus demonstrating the detection capability under different respiratory statuses.

I. INTRODUCTION

Respiration is a basic physiological activity that plays a vital role in facilitating gas exchange and metabolism and maintaining homeostasis. Accordingly, in clinical practice, respiration can provide useful information about human physiology and pathology. Nowadays, increasing air pollution and the worldwide COVID-19 pandemic are posing growing threats to the health of people, and therefore, respiration detection has attracted increasing research attention. Respiration detection has been clinically applied to monitor the human physiological state and diagnose various respiratory diseases. Therefore, it makes sense if respiration can be detected by a simple, applicable, and accurate method.

Many studies so far have investigated respiration detection. The detection methods are generally divided into three categories: motion-based, airflow-based, and autonomic nervous system (ANS) activity-based methods. In motion-based methods, various types of sensors have been applied to detect the periodic movement of the human body owing to respiration. For example, a piezoelectric poly(vinylidene fluoride) (PVDF) film [1] worked as a waistband to sense chest movements directly. A polymer optical fiber sensor [2] attached to clothes worked on the same principle. Moreover, shoulder movements were tracked with a camera to detect

¹Z. Xu, A. Furui, S. Jomyo, T. Sakagawa, and T. Tsuji are with the Graduate School of Advanced Science and Engineering, Hiroshima University, 1-4-1 Kagamiyama, Higashi-Hiroshima City, Hiroshima, 739-8527, Japan (corresponding author to provide e-mail: ziqiangxu@hiroshima-u.ac.jp).

²M. Morita, T. Takai, and M. Ando are with Murata Manufacturing Co., Ltd., Kyoto 617-8555, Japan (e-mail: masanori.morita@murata.com).

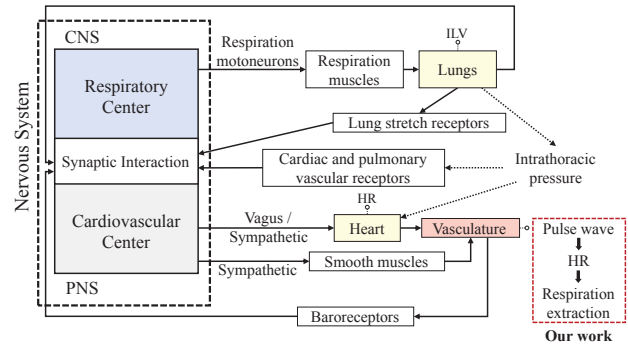


Fig. 1. Simplified model of cardiorespiratory control of respiration and cardiovascular center, and aim of the present study. CNS: central nervous system; PNS: peripheral nervous system; ILV: instantaneous lung volume; HR: heart rate.

respiration [3]. However, abnormal body movements can potentially add noise to the detection results and decrease the detection accuracy. Airflow-based methods mainly focus on airflow changes during respiration. For example, a chemical sensor was applied to detect the humidity of the exhalation [4]. This method is accurate in principle; however, a sensor placed near the nose or mouth may cause unpleasant sensations, and the resulting ANS activity may affect the detection results adversely.

Among ANS-activity-based methods, photoplethysmography (PPG) [5], [6] and electrocardiogram (ECG) [7] have been applied for respiration extraction based on the frequency domain characteristics or waveform features. These methods are based on synchronous changes in heart rate variability (HRV) and respiration, called respiratory sinus arrhythmia (RSA), that can reveal respiratory-circulatory interactions [8]. Notably, two branches of the ANS—the parasympathetic nervous system, and the sympathetic nervous system, have been confirmed to antagonistically control the heart [9] and be partially innervated by the central respiratory center. Simplistically, in the model shown in Fig. 1 [10], respiration can be directly associated with heart rate (HR), and therefore, HR was adopted as an indicator for respiration detection. Generally, HR can be calculated using PPG, ECG, or a pulse wave. However, PPG or ECG measurements are systematically limited by the measurement method and site compared with pulse wave measurement; in other words, they have lower applicability.

This study proposes a parallel measurement and extraction method for respiration from the HR measured using a novel biodegradable piezoelectric sensor, in accordance with

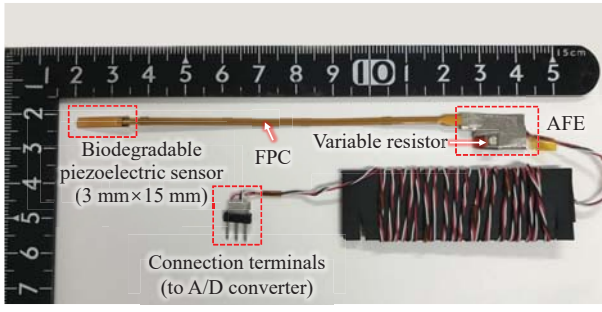


Fig. 2. Photography of a biodegradable piezoelectric sensor. FPC: flexible print circuit; AFE: analog front end, including a variable resistor for gain adjustment and a band-pass filter with low/high cut-off frequencies of 0.5 and 10 Hz, respectively.

the relationship between respiration and ANS activity. This method enables the simultaneous parallel detection of HR and respiration without imposing an additional burden on the subject. As a result, it should find broader prospects in diagnosing respiratory system diseases caused by autonomic nervous disorders and other clinical applications.

II. PROPOSED METHOD

Given the relationship between respiration and HR, in this study, pulse waves were measured using multiple piezoelectric sensors for calculating the HR. Then, the task can be translated accordingly into peak point detection of the pulse wave and respiratory feature extraction.

A. Measurement Method

To obtain a stable pulse wave, that is, an accurate HR, a biodegradable piezoelectric sensor (Murata Manufacturing Co., Ltd., Kyoto, Japan) was employed for measurements [11]. This piezoelectric film of poly(L-lactic acid) (PLLA) with a large piezoelectric constant and low dielectric constant, could respond sensitively to small deformations caused by pulse waves. More importantly, compared with the conventional piezoelectric sensors, this sensor is nonpyroelectric, and can thus avoid the heating influence of the body temperature and maintain a stable output during the measurement. In addition, the biocompatibility and biodegradability of PLLA indicate no harm to the human body and environment. Fig. 2 shows an example of a biodegradable piezoelectric sensor with a size of 3 mm×15 mm.

In this study, multiple pulse waves were measured using three biodegradable piezoelectric sensors. As shown in Fig. 3, sensors were worn on the skin at the forehead, wrist, and forefinger, where the arteries are palpable enough to measure the corresponding pulse waves to extract respiration in parallel in the experiment. Moreover, a respiratory sensor and an ECG sensor were applied as references for comparison and validation with the detection results.

B. Respiration Extraction Method

Fig. 4 shows an overview of the extraction method. Considering the connection and similarity of the pulse wave and ECG signal in terms of waveform features, the real-time

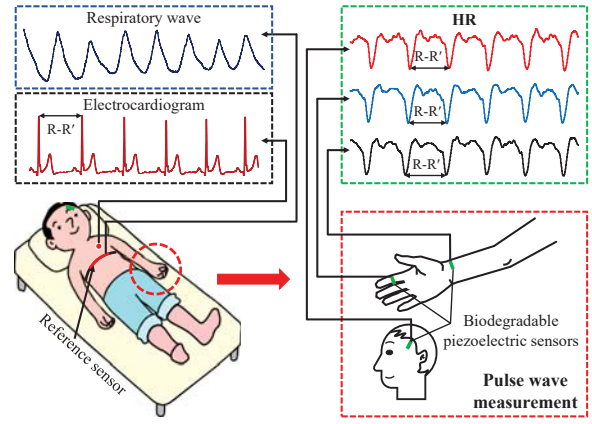


Fig. 3. Overview of the measurement method.

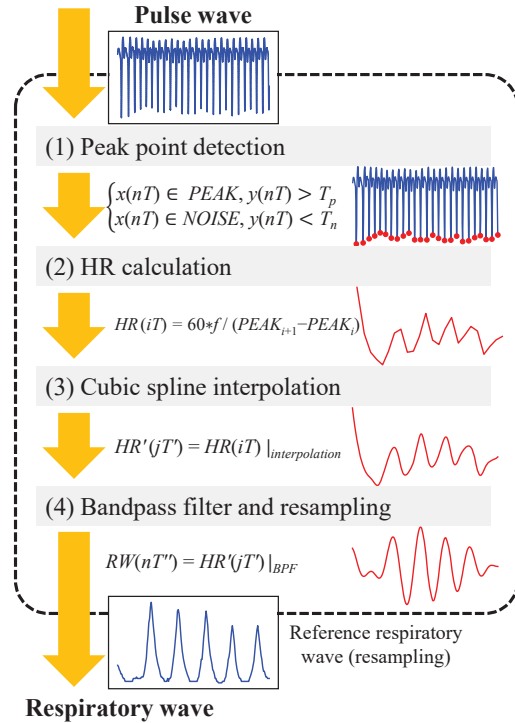


Fig. 4. Overview of respiration extraction method. *PEAK* and *NOISE*: starting point of each cycle and other peak points, respectively; T_p and T_n : peak threshold and noise threshold, respectively; N : number of the detected starting point; f and T : original sampling frequency and period, respectively; T' and T'' : interpolation period and resampling period, respectively; *RW*: respiratory wave; *BPF*: bandpass filter.

QRS detection method [12] was used to detect the starting point of each heartbeat cycle in the pulse wave.

Accordingly, HR was computed beat-by-beat by using the detected successive peak points of each pulse wave. In contrast to real-world biological signals, the current HR calculations do not vary continuously but only at specific moments. Therefore, cubic spline interpolation upsampling to 1 kHz was performed to implement and generate a continuous curve. Next, fast Fourier transform was performed on the HR interpolation results, and Fig. 5 shows one example of the analysis results. The respiratory component in the quiet state

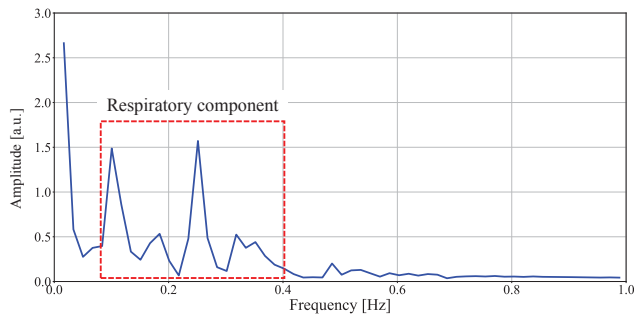


Fig. 5. Spectrum of one example of HR interpolation results.

lies in the frequency band of 0.1–0.4 Hz; that is the same as the results for the two subjects shown later but actually varies by individual. Therefore, the respiratory component can be extracted from the HR smoothly by using a corresponding bandpass filter and resampling from 1 kHz to 10 Hz.

III. EXPERIMENT

To demonstrate the detection capability of the proposed method, an experiment including several respiratory statuses simultaneously was designed and performed. Seven healthy male participants (mean age \pm SD: 23.3 \pm 1.5 years) participated in the experiments. Three of the participants were measured only for pulse waves of the arteries near the forearm to remove the influence of the head movement. All experiments were conducted in accordance with the Declaration of Helsinki. Informed consent was obtained from all study participants before the experiments were performed, and the study was approved by the Hiroshima University Ethics Committee (Registration number: E-17-2).

The pulse waves were measured using the above-described biodegradable piezoelectric sensor. The reference respiratory wave was measured using a chest breathing pickup (TR-101H and ZB-153H, NIHON KOHDEN Corp., Tokyo, Japan). A reference ECG signal was measured using a biological information monitor (BP-608EV, OMRON HEALTH-CARE Co., Ltd., Kyoto, Japan). All measured biological signals were converted and stored at 10 kHz on a PC with an A/D converter (DC-300H, NIHON KOHDEN Corp., Tokyo, Japan). For comparison, the reference respiratory wave was resampled to 10 Hz.

The Valsalva maneuver (VM) is a forced expiratory effort against a closed airway, and it involves multiple changes in respiratory status and ANS activity that can meet the requirements for experimental validation. During the experiment, each participant was placed in a supine position and wore a blindfold and noise-canceling headphones. The experimental protocol shown in Fig. 6, consists of five sequential trials, each with an interval of 2 minutes to relax the subject. Each trial starts with a 60-s rest, followed by 5 s of deep inspiration and 15 s of forced exhalation, and ends with a 60-s rest.

For comparison, the correlations between the detected results and the reference results, including HR and respiratory rate (RR), were analyzed using the linear regression method. The statistical tests using t-test for regression coefficient

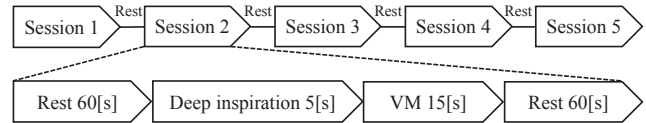


Fig. 6. Experimental protocol.

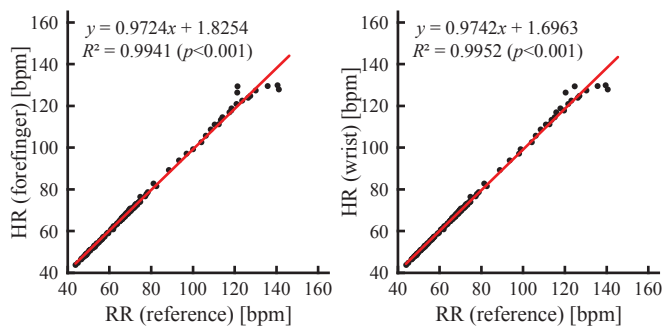
significance, especially for the slope, were carried out. In addition, Bland-Altman analysis was applied to describe the agreement between the two quantitative measurements.

IV. RESULTS AND DISCUSSION

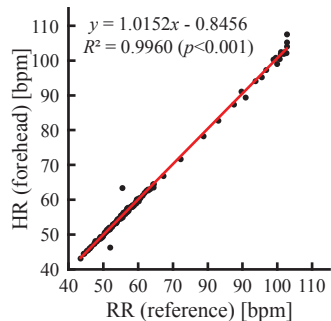
Figs. 7(a) and (c) show the relationships between the reference HR and the calculated HR from the pulse waves of arteries near the forefinger and wrist of participant A and the facial pulse wave of participant B, as well as the statistical test results using t-test (significance level: 5%) for regression coefficient significance. Figs. 7(b) and (d) show the calculated HR, extracted respiratory waves, and reference respiratory waves of participants A and B, respectively. In the quiet state (0–60 s), RR can be derived from respiratory waves; it is 18 beats per minute (bpm) in (b) and 15 bpm in (d), compared with the corresponding reference RR of 19 bpm and 15 bpm, respectively. During the deep inspiration and the VM (60–80 s), abnormal respiration and ANS activity resulted in no extraction result for respiration but reflected the ANS activity. During the respiratory recovery state (80–85 s), intense changes in inner pressure and corresponding ANS activity occurred, followed by a return to normal respiration in the subject (85–140 s).

The high consistencies ($R^2 = 0.9941, 0.9952, \text{ and } 0.9960$; $p < 0.001$) of the above HR results, as can be seen from Fig. 7, indicate that the results detected from different sites perform almost the same precision while providing a basis for accurate extraction of respiration. As expected, the respiration results extracted from multiple sites agree with each other and are generally consistent with the reference respiration results. However, the difference in HR arises from the deformed pulse waves when the VM ended. The difference in RR is due to the signal delay between the two methods with different principles, as shown in Fig. 1.

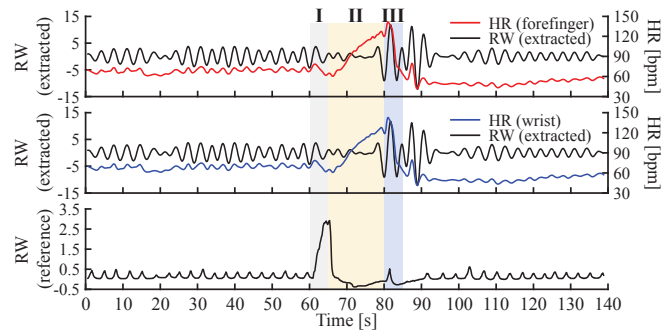
Fig. 8(a) shows the relationship between 66 pairs of detected and reference RRs in the quiet state (0–60 s) in the experiment, as well as the statistical test result using t-test (significance level: 5%) for regression coefficient significance. Fig. 8(b) shows the Bland-Altman analysis results obtained using the difference and mean values of the above two results. The plot reveals that the mean error is -0.0455 bpm with the 95% limits of agreement (LOA) ranging from -1.2079 to 1.1170 bpm, and it does not have fixed bias or proportional bias. The difference between the above two results mainly arises from the different physiological states of the different participants and the signal delay between the two methods. Overall, although the results vary from person to person, the high consistency ($R^2 = 0.9506$; $p < 0.001$) and 98.5% (65/66) of the results falling within the 95% LOA demonstrates the validity of the proposed method.



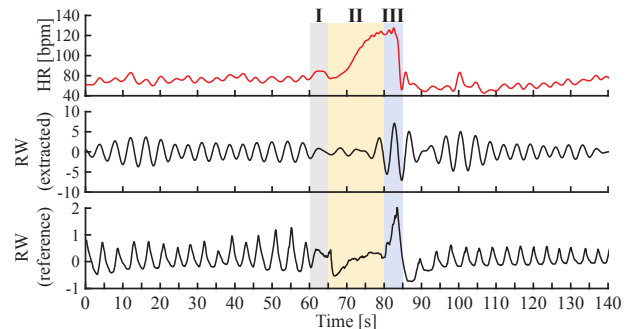
(a) Relationships between reference HR and calculated HR (participant A)



(c) Relationship between reference HR and calculated HR (participant B)



(b) Extracted HR and RW and reference RW (participant A)



(d) Extracted HR and RW and reference RW (participant B)

Fig. 7. HR and respiration detection results. I: deep inspiration; II: VM; III: respiratory recovery; RW: respiratory wave.

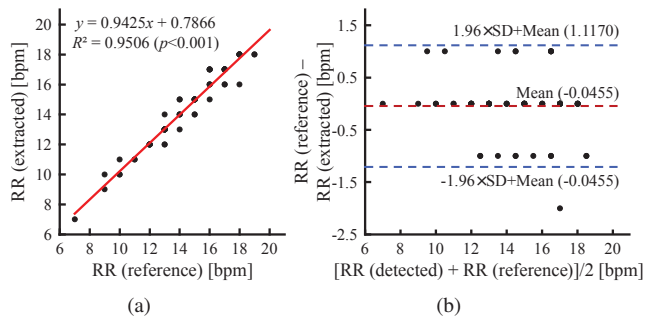


Fig. 8. Results of consistency check. (a) Relationship between detected RR and reference RR. (b) Bland-Altman analysis results. The graphs indicate the agreement of 66 pairs of measurements. The regression analysis result ($p < 0.001$) is shown with a red line. The mean error and 95% LOA are indicated with red and blue dashed lines, respectively.

V. CONCLUSIONS

In this study, based on the relationship between respiration and ANS activity, we introduced the concept of the consistency of both the HR and the resulting detected RR at different sites. A respiration detection method was designed to extract RR from the HR calculated from pulse waves at different sites using a novel biodegradable piezoelectric sensor. Compared with existing approaches, this method reduces the burden on subjects, shows high accuracy, and improves the applicability of the method, especially by supporting parallel measurements. Notably, this method is susceptible to ANS activity caused by changes in the physiological or mental state but simultaneously shows the perceptivity to

the nervous system activity. However, a major challenge for future practical applications remains distinguishing and eliminating the effects generated by anomalous ANS activity during detection.

REFERENCES

- [1] K. J. Kim *et al.*, "A novel piezoelectric PVDF film-based physiological sensing belt for a complementary respiration and heartbeat monitoring system," *Integr. Ferroelectr.*, vol. 107, no. 1, pp. 53–68, 2009.
- [2] A. G. Leal-Junior *et al.*, "Polymer optical fiber-based sensor for simultaneous measurement of breath and heart rate under dynamic movements," *Opt. Laser Technol.*, vol. 109, pp. 429–436, 2019.
- [3] D. Shao *et al.*, "Noncontact monitoring breathing pattern, exhalation flow rate and pulse transit time," *IEEE Trans. Biomed. Eng.*, vol. 61, no. 11, pp. 2760–2767, 2014.
- [4] J. Dai *et al.*, "Design strategy for ultrafast-response humidity sensors based on gel polymer electrolytes and application for detecting respiration," *Sens. Actuators, B*, vol. 304, pp. 127270, 2020.
- [5] S. Fleming and L. Tarassenko, "A comparison of signal processing techniques for the extraction of breathing rate from the photoplethysmogram," *Int J Biol Med Sci*, vol. 2, 2007.
- [6] J. Lazaro *et al.*, "Deriving respiration from photoplethysmographic pulse width," *Med. Biol. Eng. Comput.*, vol. 51, pp. 233–242, 2013.
- [7] B. Aysin and E. Aysin, "Effect of respiration in heart rate variability (HRV) analysis," in *Conf Proc IEEE Eng Med Biol Soc. 2006*, pp. 1776–1779, 2006.
- [8] F. Yasuma and J. ichiro Hayano, "Respiratory sinus arrhythmia: why does the heartbeat synchronize with respiratory rhythm?," *Chest*, vol. 125, pp. 683–690, 2004.
- [9] H. B. Hopf *et al.*, "Low-frequency spectral power of heart rate variability is not a specific marker of cardiac sympathetic modulation," *Anesthesiology*, vol. 82, pp. 609–619, 1995.
- [10] M. Russo *et al.*, "The physiological effects of slow breathing in the healthy human," *Breathe*, vol. 13, pp. 298–309, 12 2017.
- [11] M. Ando *et al.*, "Film sensor device fabricated by a piezoelectric poly(L-lactic acid) film," *Jpn. J. Appl. Phys.*, vol. 51, 2012.
- [12] J. Pan and W. J. Tompkins, "A real-time QRS detection algorithm," *IEEE Trans. Biomed. Eng.*, vol. BME-32, no. 3, pp. 230–236, 1985.